Eur. Phys. J. C (2017) 77:131
DOI 10.1140/epjc/s10052-017-4691-2

THE EUROPEAN PHYSICAL JOURNAL C

CrossMark

Regular Article - Theoretical Physics

Warm modified Chaplygin gas shaft inflation

Abdul Jawad[a], **Amara Ilyas**[b], **Shamaila Rani**[c]

Department of Mathematics, COMSATS Institute of Information Technology, Lahore 54000, Pakistan

Received: 8 September 2016 / Accepted: 19 January 2017 / Published online: 25 February 2017
© The Author(s) 2017. This article is published with open access at Springerlink.com

Abstract In this paper, we examine the possible realization of a new inflation family called "shaft inflation" by assuming the modified Chaplygin gas model and a tachyon scalar field. We also consider the special form of the dissipative coefficient $\Gamma = a_0 \frac{T^3}{\phi^2}$ and calculate the various inflationary parameters in the scenario of strong and weak dissipative regimes. In order to examine the behavior of inflationary parameters, the n_s–ϕ, n_s–r, and n_s–α_s planes (where n_s, α_s, r, and ϕ represent the spectral index, its running, tensor-to-scalar ratio, and scalar field, respectively) are being developed, which lead to the constraints $r < 0.11$, $n_s = 0.96 \pm 0.025$, and $\alpha_s = -0.019 \pm 0.025$. It is quite interesting that these results of the inflationary parameters are compatible with BICEP2, WMAP $(7+9)$ and recent Planck data.

1 Introduction

Inflation is the most acceptable paradigm that describes the physics of the very early universe. Besides solving most of the shortcomings of the hot big-bang scenario, like the horizon, the flatness, and the monopole problems [1–6], inflation also generates a mechanism to explain the large-scale structure (LSS) of the universe [7–11] and the origin of the anisotropies observed in the cosmic microwave background (CMB) radiation [12–19]. The primordial density perturbations may be sourced from quantum fluctuations of the inflaton scalar field during the inflationary expansion. The standard cold inflation scenario is divided into two regimes: the slow-roll and reheating phases. In the slow-roll period, the universe undergoes an accelerated expansion and all interactions between the inflaton scalar field and other fields' degrees of freedom are typically neglected. Subsequently, a reheating period [20,21] is invoked to end the brief acceleration. After reheating, the universe is filled with relativistic particles and thus the universe enters in the radiation big-bang epoch. For a modern review of reheating, see [22].

On the other hand, warm inflation is an alternative mechanism for having successful inflation. The warm inflation scenario, as opposed to standard cold inflation, has the essential feature that a reheating phase is avoided at the end of the accelerated expansion due to the decay of the inflaton into radiation and particles during the slow-roll phase [23–25]. During warm inflation, the temperature of the universe did not drop dramatically and the universe can smoothly enter into the decelerated, radiation-dominated period, which is essential for successful big-bang nucleosynthesis. In the warm inflation scenario, dissipative effects are important during the accelerated expansion, so that radiation production occurs concurrently with the accelerated expansion. The dissipative effect arises from a friction term Γ which describes the processes of the scalar field dissipating into a thermal bath via its interaction with other fields' degrees of freedom.

The effectiveness of warm inflation may be parameterized by the ratio $R \equiv \Gamma/3H$. The weak dissipative regime for warm inflation is for $R \ll 1$, while for $R \gg 1$, it is the strong dissipative regime. Following Refs. [26,27], the general parametrization of the dissipative coefficient depending on both the temperature of the thermal bath T and the inflaton scalar field ϕ can be written as

$$\Gamma(T,\phi) = C_\phi \frac{T^m}{\phi^{m-1}}, \tag{1}$$

where the parameter C_ϕ is related with the dissipative microscopic dynamics, the exponent m is an integer whose value is depends on the specifics of the model construction for warm inflation and on the temperature regime of the thermal bath.

[a] e-mails: jawadab181@yahoo.com; abduljawad@ciitlahore.edu.pk
[b] e-mail: amara_Ilyas14@yahoo.com
[c] e-mails: shamailatoor.math@yahoo.com; drshamailarani@ciitlahore.edu.pk

Typically, it is found that $m = 3$ (low temperature), $m = 1$ (high temperature) or $m = 0$ (constant dissipation).

Later on, Linde [28] introduced the chaotic inflation by realizing that the initial conditions for scalar field driving inflation which may help in solving the persisting inflationary problems. A plethora of work in the subject of warm inflation along with the chaotic potential has been done. For instance, Herrera [29] investigated the warm inflation in the presence of chaotic potential in loop quantum cosmology and found consistencies of the results with the observational data. Del campo and Herrera [30] discussed the warm inflationary model in the presence of a standard scalar field, the dissipation coefficient of the form $\Gamma \propto \phi^n$, and the generalized Chaplygin gas (GCG); one extracted various inflationary parameters. Setare and Kamali investigated warm tachyon inflation by assuming intermediate [31] and logamediate scenarios [32]. Bastero-Gill et al. [33] obtained the expressions for the dissipation coefficient in supersymmetric (SUSY) models and their result provides possibilities for realization of warm inflation in SUSY field theories. Bastero-Gill et al. [34] have also explored inflation by assuming the quartic potential. Herrera et al. [35] studied intermediate inflation in the context of GCG using standard and tachyon scalar field.

Panotopoulos and Vidaela [36] discussed the warm inflation by assuming quartic potential and decay rate proportional to temperature and found that the results of inflationary parameters are compatible with the latest Planck data. Moreover, many authors have investigated the warm inflation in various alternative as well as modified theories of gravity [37–49]. Recently, a new family of inflation models is being developed named shaft inflation [50]. The idea of this inflation was that the inflationary flatness is effected by a shaft i.e; when the scalar field found itself nearest to one of them, it slow-rolls inside the shaft, until inflation ends and gives way to hot big bang cosmology. The generalized form of the shaft potential is

$$V(\phi) = \frac{M_p^4 \phi^{2n-2}}{(\phi^n + m^n)^{2-\frac{2}{n}}}, \tag{2}$$

where M_p, m, n are massless constants.

In the present article, we discuss warm inflation by assuming a shaft potential, a modified Chaplygin gas model, and the tachyon scalar field. We will extract the inflationary parameters. The format of the paper is as follows: in the next section, we will discuss the detailed inflationary scenario with a tachyon field and generalized dissipative coefficient. Sections 3 and 4 contain the information as regards disordered parameters for the shaft potential in the strong and weak dissipative regimes, respectively. In Sect. 5, the results are given in summarized form.

2 Tachyon scalar field inflationary scenario

The universe undergoes an accelerated expansion of the universe. Responsible for this acceleration of the late expansion is an exotic component having a negative pressure, usually known as dark energy (DE). Several models have been already proposed as DE candidates, such as the cosmological constant [51], quintessence [52–54], k-essence [55–57], the tachyon [58–60], phantom [61–63], Chaplygin gas [64], and holographic dark energy [65], among others in order to modify the matter sector of the gravitational action. Despite the abundance of models, the nature of the dark sector of the universe, i.e. DE and dark matter, is still unknown. There exists another way of understanding the observed universe in which dark matter and DE are described by a single unified component. Particularly, the Chaplygin gas [64] achieves the unification of DE and dark matter. In this sense, the Chaplygin gas behaves as a pressureless matter at the early times and like a cosmological constant at late times. The original Chaplygin gas is characterized by an exotic equation of state with negative pressure,

$$p = -\frac{\beta}{\rho}, \tag{3}$$

whit β being a constant parameter. The original Chaplygin gas has been extended to the so-called generalized Chaplygin gas (GCG) with the following equation of state [66]:

$$p_{gcg} = -\frac{\beta}{\rho^\sigma}, \tag{4}$$

with $0 \leq \sigma \leq 1$. For the particular case $\lambda = 1$, the original Chaplygin gas is recovered. The main motivation for studying this kind of model comes from string theory. The Chaplygin gas emerges as an effective fluid associated with D-branes which may be obtained from the Born–Infeld action [67]. At background level, the GCG is able to describe the cosmological dynamics [68], however, the model presents serious issues at perturbative level [69]. Thus, a modification to the GCG results in the modified Chaplygin gas (MCG) with an equation of state given by [70]

$$p = \omega\rho - \frac{\beta}{\rho^\sigma}, \tag{5}$$

where ω is a constant parameter, with $0 \leq \sigma \leq 1$, is suitable to describe the evolution of the universe [71,72] which is also consistent with perturbative study [73].

The energy conservation equation for the MCG model turns out to be

$$\rho_{mcg} = \left(\frac{\beta}{1+\omega} + \frac{\upsilon}{a^{3(1+\sigma)(1+\omega)}}\right)^{\frac{1}{1+\sigma}}, \tag{6}$$

where υ is a constant of integration. In a spatially flat FRW model, the Friedmann equation is described by

$$H^2 = \frac{1}{3M_p^2}(\rho_m + \rho_\gamma), \tag{7}$$

where ρ_m is the energy density of the matter field and ρ_γ is the energy density of the radiation field. The warm MCG model modifies the first Friedmann equation which has been used in Eq. (7); it reduces to

$$H^2 = \frac{1}{3M_p^2}\left[\left(\frac{\beta}{1+\omega} + \upsilon\rho_\phi^{(1+\sigma)(1+\omega)}\right)^{\frac{1}{1+\sigma}} + \rho_\gamma\right], \tag{8}$$

which is named Chaplygin gas inspired inflation. The energy density and pressure of tachyon scalar field are defined as follows [74]:

$$\rho_\phi = \frac{V(\phi)}{\sqrt{1-\dot\phi^2}}, \quad p_\phi = -V(\phi)\sqrt{1-\dot\phi^2}. \tag{9}$$

The inflaton and imperfect fluid energy densities according to Eq. (9) are conserved as

$$\dot\rho_\phi + 3H(\rho_\phi + p_\phi) = -\Gamma\dot\phi^2, \tag{10}$$

$$\dot\rho_\gamma + 4H\rho_\gamma = \Gamma\dot\phi^2, \tag{11}$$

where Γ is the dissipation factor that evaluates the rate of decay of ρ_ϕ into ρ_γ. It is also important to note that this decay rate can be used as a function of the temperature of the thermal bath and the scalar field, i.e., $\Gamma(T,\phi)$, or a function of only the temperature of the thermal bath $\Gamma(T)$, or a function of scalar field only, $\Gamma(\phi)$, or simply a constant.

The second law of thermodynamics indicates that Γ must be positive, so the inflaton energy density decomposes into radiation density. The second conservation equation is given by

$$\begin{aligned}
&\frac{\ddot\phi}{1-\dot\phi^2} + 3H\dot\phi + \frac{V'(\phi)}{V(\phi)} = -\frac{\Gamma\dot\phi}{V}\sqrt{1-\dot\phi^2},\\
&\Rightarrow \ddot\phi + \left(3H + \frac{\Gamma}{V}\right)\dot\phi = -\frac{V'(\phi)}{V(\phi)}, \quad \dot\phi \ll 1\\
&\Rightarrow 3H(1+R)\dot\phi = -\frac{V'(\phi)}{V(\phi)}, \quad \text{where} \quad \ddot\phi \ll \left(3H + \frac{\Gamma}{V}\right)\dot\phi,
\end{aligned} \tag{12}$$

where $R = \frac{\Gamma}{3HV}$. In a weak dissipative epoch, $R \ll 1$ leads to $\Gamma \ll 3H$, while $R \gg 1$ indicates the high dissipative regime. Here, we assume some constraints, which lead to a static epoch, i.e., $\rho_\phi \approx V(\phi)$, the slow-roll limit, $V(\phi) \gg \dot\phi^2$, $(3H+\Gamma)\dot\phi \gg \ddot\phi$, and quasi-stable decay of ρ_ϕ into ρ_γ, $4H\rho_\gamma \gg \dot\rho_\gamma$ and $\Gamma\dot\phi^2 \gg \dot\rho_\gamma$. As is well known the energy density of the scalar field is much greater than the energy density of radiation but also, at the same time, the energy can be larger than the expansion rate with $\rho_\gamma^{\frac{1}{4}} > H$. This is approximately equal to $T > H$ by considering thermalization, which is the true condition as regards warm inflation. With the help of all these limits Eqs. (7), (11), and (12) become

$$H^2 = \frac{1}{3M_p^2}\left(\frac{\beta}{1+\omega} + \upsilon\rho_\phi^{(1+\sigma)(1+\omega)}\right)^{\frac{1}{1+\sigma}}, \tag{13}$$

$$4H\rho_\gamma = \Gamma\dot\phi^2, \tag{14}$$

$$3H(1+R)\dot\phi = -\frac{V'(\phi)}{V(\phi)}, \tag{15}$$

where a prime represents the derivative with respect to ϕ.

The energy density of radiation can be used as $C_\gamma T^4$ when we have taken the thermalization. Here $C_\gamma = \pi^2 g_*/30$, where g_* shows the degree of freedom. This expression gives the value as $C_\gamma \simeq 70$ with $g_* = 228.75$. The temperature of the thermal bath can be obtained by merging Eqs. (14) and (15),

$$T = \left(\frac{\Gamma V'^2}{36C_\gamma H^3 V^2(1+R)^2}\right)^{\frac{1}{4}}, \tag{16}$$

where $\Gamma = a_0\frac{T^q}{\phi^{q-1}}$, which is the general form of the dissipative coefficient, while a_0 and q are constant parameters associated with dissipative microscopic dynamics. The consequences of radiation are studied during inflation through this kind of dynamic which was suggested for the first time in warm inflation with the theoretical basis of supersymmetry (SUSY) [75,76].

A set of dimensionless slow-roll parameters must be satisfied for the occurrence of warm inflation which are defined in the form of the Hubble parameter as [77]

$$\epsilon = -\frac{\dot H}{H^2}, \quad \eta = -\frac{\ddot H}{H\dot H}.$$

The slow-roll parameters can also be deduced in the form of scalar field and thermalization according to the tachyon field along with modified Chaplygin gas, which are defined as

$$\epsilon = \frac{\upsilon(1+\omega)M_p^2 V^{(1+\sigma)(1+\omega)-2}V'^2}{2(1+R)\left(\frac{\beta}{1+\omega} + \upsilon V^{(1+\sigma)(1+\omega)}\right)^{1+\frac{1}{1+\sigma}}},$$

$$\eta = \frac{M_p^2}{(1+R)\left(\frac{\beta}{1+\omega} + \upsilon V^{(1+\sigma)(1+\omega)}\right)^{\frac{1}{1+\sigma}}} \times\left[\frac{((1+\sigma)(1+\omega)-2)V'^2}{V^2} + \frac{2V''}{V}\right] - 2(1+\sigma)\epsilon.$$

We can describe number of e-folds in terms of the Hubble parameter as well as the inflaton

$$N(\phi) = \int_{t_i}^{t_f} H\mathrm{d}t = \int_{\phi_i}^{\phi_f} \frac{H}{\dot{\phi}}\mathrm{d}\phi, \tag{17}$$

where ϕ_i and ϕ_f can be calculated with the help of first and second slow-roll parametric conditions, i.e., $\epsilon = 1 + R$ and $|\eta| = 1 + R$.

Next, we will calculate some inflationary parameters such as tensor and scalar power spectra (P_R, P_g), tensor and scalar spectral indices (n_R, n_s). The form of the scalar power spectrum can be estimated as $P_R(k_0) \equiv \frac{25}{4}\delta_H^2(k_0)$, where we have the density disorders $\delta_H^2(k_0) \equiv \frac{k_F(T_R)}{2\pi^2}$ and $k_F = \sqrt{\Gamma H}$. However, the amplitude of the tensor and scalar power spectrum of the curvature perturbation are given by

$$P_R \simeq \left(\frac{H}{2\pi}\right)^2 \left(\frac{3H^2}{V'}\right)^2 \left(\frac{T}{H}\right)(1+R)^{\frac{5}{2}},$$
$$P_g \simeq 24\kappa \left(\frac{H}{2\pi}\right)^2. \tag{18}$$

The tensor-to-scalar ratio can be computed by using the relation $r = \frac{P_R}{P_g}$. However, the spectral index and running of the spectral index are defined as [78]

$$n_s = 1 + \frac{d\ln P_R}{d\ln k}, \quad \alpha_s = \frac{\mathrm{d}n_s}{d\ln k}. \tag{19}$$

Here, the interval in wave number k is referred to the number of e-folds N, through the expression

$$d\ln k = -\mathrm{d}N. \tag{20}$$

In the following, we will evaluate the inflationary parameters for the weak and strong dissipative regimes.

3 Inflationary parameters in the strong epoch with shaft potential

The special case of the shaft potential where $n = 2$ is considered for which Eq. (2) takes the form $V(\phi) = \frac{M_p^4\phi^2}{(\phi^2+m^2)}$. The temperature of the radiation for the present model with the help of the shaft potential, Eq. (16), takes the following form:

$$T = \left(\frac{m^6 M_p^5 \sqrt{3\left(\frac{\beta}{1+\omega} + \upsilon\left(\frac{M_p^4\phi^2}{m^2+\phi^2}\right)^{(1+\omega)(1+\sigma)}\right)^{-\frac{1}{1+\sigma}}}}{a_0(m^2+\phi^2)^3\left(M_p^4 - \frac{M_p^4\phi^2}{m^2+\phi^2}\right)C_\gamma}\right)^{\frac{1}{7}}. \tag{21}$$

The number of e-folds can be calculated by Eq. (17) with $\dot{\phi} = \frac{-V'}{3HVR}$ for the strong regime as

$$N = \frac{a_0^{\frac{4}{7}}}{23^{2/7} m^{\frac{2}{7}} M_p^{\frac{4}{7}}} \times \int_{\phi_i}^{\phi_f} \left(\sqrt{\left(\frac{\beta}{1+\omega} + \upsilon\left(\frac{M_p^4\phi^2}{m^2+\phi^2}\right)^{(1+\omega)(1+\sigma)}\right)^{\frac{1}{1+\sigma}}}\right)^{\frac{10}{7}} \times \left(\frac{(m^2+\phi^2)^{\frac{1}{7}}}{C_\gamma^{3/7}\phi}\right)\mathrm{d}\phi. \tag{22}$$

For the strong epoch, ϕ_i and ϕ_f can be described by considering $\epsilon = R$ and $|\eta| = R$, respectively. The power spectrum attains the value from Eq. (18) as follows:

$$P_R = \frac{a_0^{10/7}\left(\frac{m^2 M_p^4}{m^2+\phi^2}\right)^{10/7}}{483^{3/14}\pi^2 C_\gamma^{15/14}} \times \left(\frac{\left(\frac{\beta}{1+\omega} + \upsilon\left(\frac{M_p^4\phi^2}{g^2+\phi^2}\right)^{(1+\omega)(1+\sigma)}\right)^{\frac{1}{2(1+\sigma)}}}{M_p}\right)^{10/7} \times \left(\frac{\left(\frac{m^2 M_p^4\phi}{(m^2+\phi^2)^2}\right)^{1/7}}{m^{20/7}\left(\frac{M_p^4\phi^2}{m^2+\phi^2}\right)^{25/7}}\right).$$

The scalar power spectrum is given by

$$P_g = \frac{2}{9\pi M_p^4}\left(\frac{\beta}{1+\omega} + \upsilon V^{(1+\sigma)(1+\omega)}\right)^{\frac{1}{1+\sigma}}. \tag{23}$$

The tensor-to-scalar ratio can be found by using Eq. (23), which yields

$$r = \frac{32m^2 M_p^5 \upsilon\phi\left(\frac{m^2 M_p^4\phi}{(m^2+\phi^2)^2}\right)^{15/7}\left(\frac{M_p^4\phi^2}{m^2+\phi^2}\right)^{\frac{3}{7}+\omega+\sigma+\omega\sigma} 3^{2/7}(1+\omega)a_0 C_\gamma^{3/7}}{\left(\frac{a_0 m^4 M_p^4}{m^2+\phi^2}\right)^{11/7}\left(\upsilon\left(\frac{M_p^4\phi^2}{m^2+\phi^2}\right)^{(1+\sigma)(1+\omega)} + \frac{\beta}{1+\omega}\right)^{1+\frac{1}{2(1+\sigma)}}} \times \left(\frac{\left(\upsilon\left(\frac{M_p^4\phi^2}{m^2+\phi^2}\right)^{(1+\sigma)(1+\omega)} + \frac{\beta}{1+\omega}\right)^{\frac{1}{2+2\sigma}}}{M_p}\right)^{3/7}.$$

Figure 1 shows the plot of the tensor-to-scalar ratio versus spectral index within the strong regime. This ratio is being plotted for three different values of m with the condition $m < \phi$. The red line has been plotted for $m = 0.2$, the

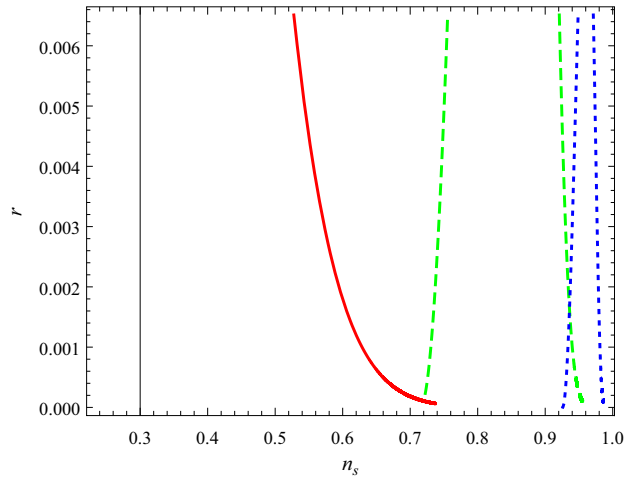

Fig. 1 Plot of the tensor-to-scalar ratio verses spectral index in the strong epoch with $a_0 = 2 \times 10^6$

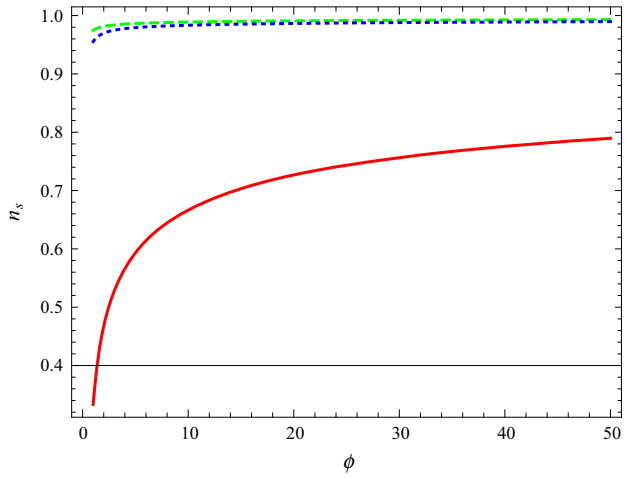

Fig. 2 Plot of the spectral index number w.r.t. inflaton in the strong epoch with $a_0 = 2 \times 10^6$

green dashed line for $m = 0.5$ and the blue dotted line for $m = 0.9$. According to the plot, the ratio is not satisfied with spectral index when $m = 0.2$, while the tensor-to-scalar ratio is compatible with the spectral index for the other two values.

However, the spectral index and its running by using Eqs. (19) and (20) attained the values

$$n_s = 1 - \left(\frac{23^{2/7}\phi^3 C_\gamma^{3/7} M_p^8 \left(\frac{m^4 a_0 M_p^4}{m^2+\phi^2}\right)^{3/7}}{7\left(m^2+\phi^2\right)^5 a_0 \left(\frac{m^2\phi M_p^4}{(m^2+\phi^2)^2}\right)^{13/7} \left(\frac{\beta}{1+\omega} + \upsilon \left(\frac{\phi^2 M_p^4}{m^2+\phi^2}\right)^{(1+\sigma)(1+\omega)}\right)} \right) \times \frac{\left(\frac{\beta(49m^2+23\phi^2)}{1+\omega} - \upsilon\left(-23\phi^2+m^2(-39+10\omega)\right)\left(\frac{\phi^2 M_p^4}{m^2+\phi^2}\right)^{(1+\sigma)(1+\omega)}\right)}{\left(\frac{\phi^2 M_p^3 \left(\frac{\beta}{1+\omega}+\upsilon\left(\frac{\phi^2 M_p^4}{m^2+\phi^2}\right)^{(1+\sigma)(1+\omega)}\right)^{\frac{1}{2+2\sigma}}}{m^2+\phi^2}\right)^{4/7}}.$$

We plot spectral index n_s versus scalar field ϕ in Fig. 2 and notice that the red line which represents the behavior of spectral index with respect to ϕ for $m = 0.2$ requires a very large value of ϕ to reach in the range of the spectral index. The other two different values i.e., $m = 0.5$ and $m = 0.9$,with green and blue lines, respectively, satisfy the range of the spectral index for $\phi \in [1, 50]$. It can be observed that the tensor-to-scalar ratio (r) remains less than 0.11 for the range of the spectral index $0.96 < n_s < 0.97$ in the strong dissipative epoch.

The running of the spectral index becomes

$$\begin{aligned}\alpha_s = -\Bigg[& 83^{4/7}\phi C_\gamma^{6/7}\left(\frac{m^2\phi M_p^4}{(m^2+\phi^2)^2}\right)^{9/7} \\ & \times\left(\frac{m^4 a_0 M_p^4}{m^2+\phi^2}\right)^{6/7}\Bigg(\left(\frac{\beta}{1+\omega}\right)^2(231m^2\phi^2 \\ & +23\phi^4) + 2\frac{\upsilon\beta}{1+\omega}(23\phi^4 + m^2\phi^2(214-17\omega) \\ & +7m^4(1+\omega)(12+5\omega+5\sigma \\ & \times(1+\omega)))\left(\frac{\phi^2 M_p^4}{m^2+\phi^2}\right)^{(1+\sigma)(1+\omega)} \\ & +\upsilon^2(23\phi^4 + m^2\phi^2(197-34\omega) - 2m^4 \\ & \times(1+\omega)(-39+10\omega))\left(\frac{\phi^2 M_p^4}{m^2+\phi^2}\right)^{2(1+\sigma)(1+\omega)}\Bigg)\Bigg] \\ & \times(49m^{10}a_0^2 M_p^4)^{-1}\left(\frac{\beta}{1+\omega}+\upsilon\left(\frac{\phi^2 M_p^4}{m^2+\phi^2}\right)^{(1+\sigma)(1+\omega)}\right)^{-2} \\ & \times\left(\frac{\phi^2 M_p^3\left(\frac{\beta}{1+\omega}+\upsilon\left(\frac{\phi^2 M_p^4}{m^2+\phi^2}\right)^{(1+\sigma)(1+\omega)}\right)^{\frac{1}{2+2\sigma}}}{m^2+\phi^2}\right)^{-8/7}.\end{aligned}$$

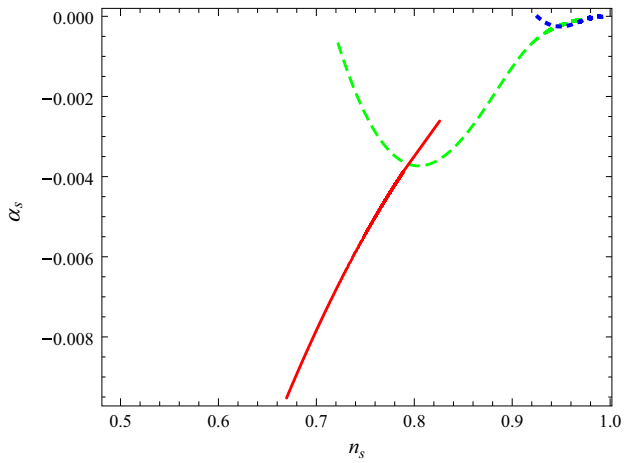

Fig. 3 Plot for the running of the spectral index versus spectral index in the strong epoch with $a_0 = 2 \times 10^6$

The plot of the running of the spectral index with respect to scalar field is shown in Fig. 3. The suggested values for the running of spectral index by WMAP7 [79,80] and WMAP9 [81] are approximately equal to -0.992 ± 0.019

and -0.019 ± 0.025, respectively. It can be observed that this parameter is compatible with the observational data for $m = 0.5$ and $m = 0.9$. However, for $m = 0.2$, the plot of the running of the spectral index is not compatible with the required range of the spectral index.

4 Inflationary parameters in the weak epoch with shaft potential

Here we study the tachyon model in the weak epoch ($R \ll 1$), the temperature of the radiation for present model with the help of the shaft potential, Eq. (21) takes the form

$$T = \frac{a_0 m^4 M_p^3 \left(\frac{\beta}{1+\omega} + \upsilon \left(\frac{\phi^2 M_p^4}{m^2+\phi^2}\right)^{(1+\sigma)(1+\omega)}\right)^{-\frac{3}{2(1+\sigma)}}}{\sqrt{3}\phi^4 (m^2+\phi^2)^2 C_\gamma}. \tag{24}$$

The number of e-folds can be calculated by Eq. (17) with $\dot{\phi} = \frac{-V'}{3HV}$ as

$$N = \frac{1}{2m^2 M_p^2} \int_{\phi_i}^{\phi_f} \times \left(\frac{\beta}{1+\omega} + \upsilon \left(\frac{\phi^2 M_p^4}{m^2+\phi^2}\right)^{(1+\sigma)(1+\omega)}\right)^{\frac{1}{1+\sigma}} \times (m^2+\phi^2)\phi \mathrm{d}\phi,$$

where ϕ_i and ϕ_f can be found by taking $\epsilon = 1$ and $|\eta| = 1$, respectively.

The power spectrum attains the value from Eq. (18)

$$P_r = \frac{(m^2+\phi^2)^3 a_0}{48 m^2 \pi^2 \phi^6 C_\gamma M_p^{14}} \left[M_p^4 - \frac{\phi^2 M_p^4}{m^2+\phi^2}\right] \times \left[\frac{\beta}{1+\omega} + \upsilon \left(\frac{\phi^2 M_p^4}{m^2+\phi^2}\right)^{(1+\sigma)(1+\omega)}\right]^{\frac{1}{1+\sigma}}.$$

The scalar power spectrum remains same as for the strong regime. The tensor-to-scalar ratio is obtained by using expressions of power spectrum and scalar spectrum, which is given by

$$r = \frac{8M_p^2(1+\omega)\upsilon}{\left(\frac{M_p^4\phi^2}{m^2+\phi^2}\right)^{2-(1+\omega)(1+\sigma)}} \left(\frac{2M_p^4\phi}{m^2+\phi^2} - \frac{2M_p^4\phi^3}{(m^2+\phi^2)^2}\right)^2 \times \left(\frac{\beta}{1+\omega} + \upsilon \left(\frac{M_p^4\phi^2}{m^2+\phi^2}\right)^{(1+\omega)(1+\sigma)}\right)^{-1-\frac{1}{1+\sigma}}.$$

Figure 4 shows the plot of the tensor-to-scalar ratio versus spectral index within weak regime. The tensor-to-scalar ratio

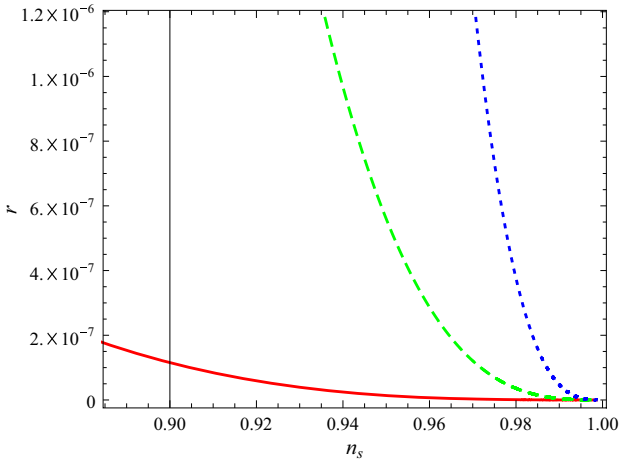

Fig. 4 Plot of the tensor-to-scalar ratio versus spectral index in the weak epoch with $a_0 = 2 \times 10^6$

is plotted for three different values of m with the condition $m < \phi$. The red line has been plotted for $m = 0.2$, the green dashed line for $m = 0.5$, and the blue dotted line for $m = 0.9$. According to the plot, there is no change in the behavior of the tensor-to-scalar ratio for the spectral index, while the tensor-to-scalar ratio is compatible with the spectral index for all values of m.

The value of the spectral index is found with the help of the above mentioned power spectrum along with the first part of Eqs. (19) and (20). It is given as follows:

$$n_s = 1 + \left(\frac{\beta}{1+\omega} + \upsilon\left(\frac{M_p^4\phi^2}{m^2+\phi^2}\right)^{(1+\omega)(1+\sigma)}\right)^{\frac{-1}{1+\sigma}} \times \left[\frac{8m^6 M_p^{10}(1+\omega)\upsilon\phi}{(m^2+\phi^2)^5} \times \left(\frac{M_p^4\phi^2}{m^2+\phi^2}\right)^{(1+\omega)(1+\sigma)} \left(\frac{\beta}{1+\omega} + \upsilon\left(\frac{M_p^4\phi^2}{m^2+\phi^2}\right)^{(1+\omega)(1+\sigma)}\right)^{-1} - \frac{4M_p^2}{(m^2+\phi^2)^3}(m^4(1+2M_p^4) + 2m^2\phi^2 + \phi^4)\right]. \tag{25}$$

Figure 5 represents the spectral index versus scalar field for $m = 0.2$, $m = 0.5$ and $m = 0.9$. According to WMAP7 [79,80], WMAP9 [81], and Planck 2015 [82], the value of the spectral index lies in the ranges 0.967 ± 0.014, 0.972 ± 0.013 and 0.968 ± 0.006.

Using Eqs. (25) and (20), the running of the spectral index is calculated as

$$\alpha_s = \frac{32m^4 M_p^8}{\phi(m^2+\phi^2)^{11}} \times \left(\frac{\beta}{1+\omega} + \upsilon\left(\frac{M_p^4\phi^2}{m^2+\phi^2}\right)^{(1+\sigma)(1+\omega)}\right)^{\frac{-2(2+\sigma)}{1+\sigma}} \times \left[\left(\frac{\beta}{1+\omega}\right)^2 \phi^2 (m^2+\phi^2)^4 (m^4(1+6M_p^4)\right.$$

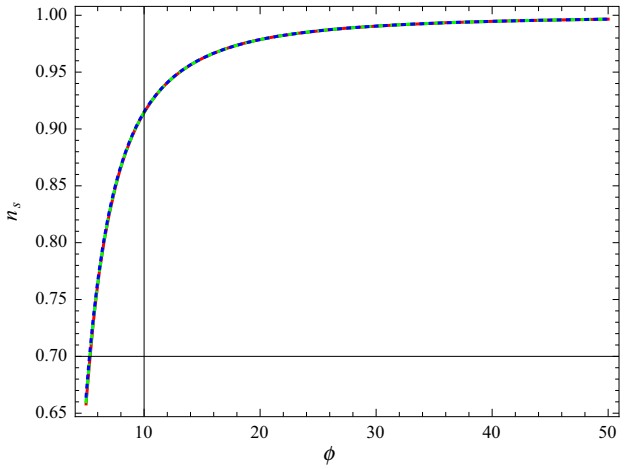

Fig. 5 Plot of the spectral index number w.r.t. inflaton in the weak epoch with $a_0 = 2 \times 10^6$

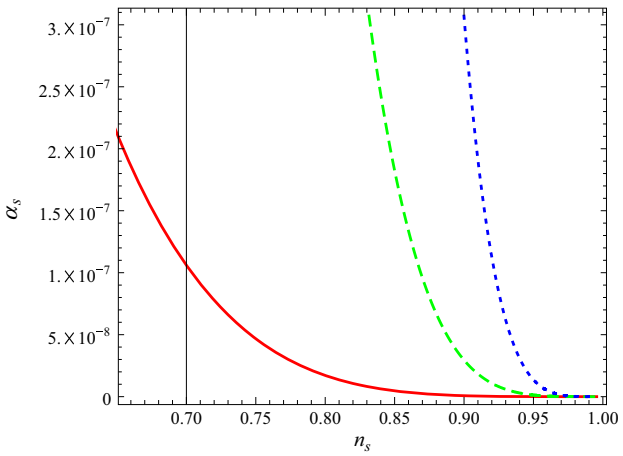

Fig. 6 Plot for the running of the spectral index versus spectral index in the weak epoch with $a_0 = 2 \times 10^6$

$$
\begin{aligned}
&+2m^2\phi^2+\phi^4)+\left(\frac{M_p^4\phi^2}{m^2+\phi^2}\right)^{-1+\sigma+\omega+\sigma\omega}\\
&\times(2\phi^{10}+m^{10}(1+2M_p^4)(1+\omega)+m^2\phi^8(9+\omega)\\
&+4m^4\phi^6(4+3M_p^4\\
&+\omega)+m^8\phi(6\phi+M_p^8(1+\omega)(3+2\omega+2\sigma(1+\omega))\\
&+4\phi(\omega+M_p^4(4\\
&+\omega)))+m^6\phi^3(-9M_p^8(1+\omega)\\
&+2\phi(7+3\omega+M_p^4(13+\omega))))\frac{\upsilon\beta M_p^8\phi^4}{1+\omega}\\
&+M^8\upsilon^2\phi^4\left(\frac{M_p^4\phi^2}{m^2+\phi^2}\right)^{2(\sigma+\omega+\sigma\omega)}\\
&\times[\phi^{10}+m^{10}(1+2M_p^4)(1+\omega)+m^2\phi^8\\
&\times(5+\omega)+2m^4\phi^6(5+3M_p^4+2\omega)\\
&+m^6\phi^3(-9M_p^8(1+\omega)+2\phi(5\\
&+3\omega+M_p^4(7+\omega)))+m^8\phi[-M_p^8(1+\omega)(1+2\omega)\\
&+\phi(5+4\omega+2M_p^4(5+2\omega))]]\Big].
\end{aligned}
$$

The plot of the running of the spectral index with respect to the scalar field is shown in Fig. 6. It can be observed that the running of the spectral index is compatible with the observational data for $m = 0.2$, $m = 0.5$, and $m = 0.9$.

5 Concluding remarks

The warm MCG inflationary scenario is being investigated with the shaft potential for a tachyon scalar field. We have discussed this inflationary scenario for both (weak and strong) dissipative regimes in a flat FRW universe. We have also examined the results for some of necessary inflationary parameters such as the slow-roll parameters, number of e-folds, scalar-tensor power spectra, spectral indices, tensor-to-scalar ratio, and running of scalar spectral index. We have analyzed these parameters for the strong epoch as well as the weak regime by using the special case of the shaft potential. We have restricted constant parameters of the models according to WMAP7 results for examining the physical behavior of n_s–ϕ, n_s–R and n_s–α_s trajectories in both cases.

We have analyzed the behavior of inflationary parameters according to two dimensionless parameters (a_0, m) where the value of $a_0 = 2 \times 10^6$ remains the same for all necessary parameters. All the trajectories are plotted for three different values i.e., $m = 0.2$, $m = 0.5$, and $m = 0.9$. For the case for $m = 0.2$ in the strong epoch, the plots showed the unsuitable behavior to satisfy the required range of inflationary parameters. However, this value showed the suitable behavior for the weak regime. The standard values of the parameters are the tensor-to-scalar ratio $r < 0.36, 0.38, 0.11$, the spectral index $n_s = 0.982 \pm 0.020, 0.992 \pm 0.019, 0.9655 \pm 0.0062$ according to WMAP7 [79,80], WMAP9 [81] and Planck 2015 [82] results, respectively. In our case, the tensor-to-scalar ratio versus spectral index is compatible with this observational data (Figs. 1 and 4). Also, Figs. 3 and 6 clearly showed the compatibility of the spectral index for its running with observational data since the observational values of running of the spectral index are $\alpha_s = -0.0084 \pm 0.0082, -0.034 \pm 0.026, -0.019 \pm 0.025$ according to Planck 2015 [82], WMAP7 [79,80], and WMAP9 [81], respectively.

Open Access This article is distributed under the terms of the Creative Commons Attribution 4.0 International License (http://creativecommons.org/licenses/by/4.0/), which permits unrestricted use, distribution, and reproduction in any medium, provided you give appropriate credit to the original author(s) and the source, provide a link to the Creative Commons license, and indicate if changes were made.
Funded by SCOAP[3].

References

1. A. Guth, Phys. Rev. D **23**, 347 (1981)
2. K. Sato, Mon. Not. R. Astron. Soc. **195**, 467 (1981)
3. A.D. Linde, Phys. Lett. B **108**, 389 (1982)
4. A.D. Linde, Phys. Lett. B **129**, 177 (1983)
5. A. Albrecht, P.J. Steinhardt, Phys. Rev. Lett. **48**, 1220 (1982)
6. A.D. Linde, Phys. Lett. B **129**, 177 (1983)
7. V.F. Mukhanov, G.V. Chibisov, JETP Lett. **33**, 532 (1981)
8. S.W. Hawking, Phys. Lett. B **115**, 295 (1982)
9. A. Guth, S.-Y. Pi, Phys. Rev. Lett. **49**, 1110 (1982)
10. A.A. Starobinsky, Phys. Lett. B **117**, 175 (1982)
11. J.M. Bardeen, P.J. Steinhardt, M.S. Turner, Phys. Rev. D **28**, 679 (1983)
12. D. Larson et al., Astrophys. J. Suppl. **192**, 16 (2011)
13. C.L. Bennett et al., Astrophys. J. Suppl. **192**, 17 (2011)
14. N. Jarosik et al., Astrophys. J. Suppl. **192**, 14 (2011)
15. G. Hinshaw et al. [WMAP Collaboration], Astrophys. J. Suppl. **208**, 19 (2013)
16. P.A.R. Ade et al. [Planck Collaboration], Astron. Astrophys. **571**, A16 (2014)
17. P.A.R. Ade et al. [Planck Collaboration], Astron. Astrophys. **571**, A22 (2014)
18. P.A.R. Ade et al. [Planck Collaboration], Astron. Astrophys. **594**, A13 (2016)
19. P.A.R. Ade et al. [Planck Collaboration], Astron. Astrophys. **594**, A20 (2016)
20. L. Kofman, A.D. Linde, A.A. Starobinsky, Phys. Rev. Lett. **73**, 3195 (1994)
21. L. Kofman, A.D. Linde, A.A. Starobinsky, Phys. Rev. D **56**, 3258 (1997)
22. M.A. Amin, M.P. Hertzberg, D.I. Kaiser, J. Karouby, Int. J. Mod. Phys. D **24**, 1530003 (2014)
23. I.G. Moss, Phys. Lett. B **154**, 120 (1985)
24. A. Berera, Phys. Rev. Lett. **75**, 3218 (1995)
25. A. Berera, Phys. Rev. D **55**, 3346 (1997)
26. Y. Zhang, JCAP **0903**, 023 (2009)
27. M. Bastero-Gil, A. Berera, R.O. Ramos, J.G. Rosa, JCAP **1301**, 016 (2013)
28. A.D. Linde, Phys. Lett. B **129**, 177 (1983)
29. R. Herrera, Phys. Rev. D **81**, 123511 (2010)
30. S. Del Campo, R. Herrera, Phys. Lett. B **660**, 282 (2008)
31. M.R. Setare, V. Kamali, JCAP **08**, 034 (2012)
32. M.R. Setare, V. Kamali, Phys. Rev. D **87**, 083524 (2013)
33. M. Bastero-Gil, A. Berera, R.O. Ramos, J.G. Rosa, JCAP **1301**, 016 (2013)
34. M. Bastero-Gil, A. Berera, R.O. Ramos, J.G. Rosa, JCAP **1410**, 10053 (2014)
35. R. Herrera, M. Olivares, N. Videla, Eur. Phys. J. C **73**, 2295 (2013)
36. G. Panotopoulos, N. Videla, Eur. Phys. J. C **75**, 525 (2015)
37. A. Jawad, A. Ilyas, S. Rani, Int. J. Mod. Phys. D **26**, 1750031 (2017)
38. A. Jawad, A. Ilyas, S. Rani, Astropart. Phys. **81**, 61 (2016)
39. A. Jawad, S. Rani, S. Mohsaneen, Eur. Phys. J. Plus **131**, 234 (2016)
40. A. Jawad, S. Rani, S. Mohsaneen, Astrophys. Space Sci. **361**, 158 (2016)
41. A. Jawad, S. Butt, S. Rani, Astrophys. Space Sci. **361**, 258 (2016)
42. A. Jawad, S. Butt, S. Rani, Eur. Phys. J. C **76**, 274 (2016)
43. K. Bamba, S.D. Odintsov, Eur. Phys. J. C **76**, 18 (2016)
44. K. Bamba, S.D. Odintsov, P.V. Tretyakov, Eur. Phys. J. C **75**, 344 (2015)
45. J.C.B. Sanchez, M. Bastero-Gil, A. Berera, K. Dimopoulos, Phys. Rev. D **77**, 123527 (2008)
46. R. Herrera, Phys. Rev. D **81**, 123511 (2010)
47. R. Herrera, E. San Martin, Eur. Phys. J. C **71**, 1701 (2011)
48. R. Herrera, M. Olivares, N. Videla, Eur. Phys. J. C **73**, 2295 (2013)
49. R. Herrera, M. Olivares, N. Videla, Phys. Rev. D **88**, 063535 (2013)
50. K. Dimopoulos, Phys. Lett. B **735**, 75 (2014)
51. P.J.E. Peebles, B. Ratra, Rev. Mod. Phys. **75**, 559 (2003)
52. B. Ratra, P.J.E. Peebles, Phys. Rev. D **37**, 3406 (1988)
53. R.R. Caldwell, R. Dave, P.J. Steinhardt, Phys. Rev. Lett. **80**, 1582 (1998)
54. M. Sami, T. Padmanabhan, Phys. Rev. D **67**, 083509 (2003)
55. C. Armendariz-Picon, V. Mukhanov, P.J. Steinhardt, Phys. Rev. D **63**, 103510 (2001)
56. T. Chiba, Phys. Rev. D **66**, 063514 (2002)
57. R.J. Scherrer, Phys. Rev. Lett. **93**, 011301 (2004)
58. A. Sen, J. High Energy Phys. **04**, 048 (2002)
59. A. Sen, J. High Energy Phys. **07**, 065 (2002)
60. G.W. Gibbons, Phys. Lett. B **537**, 1 (2002)
61. R.R. Caldwell, Phys. Lett. B **545**, 23 (2002)
62. E. Elizade, S. Nojiri, S. Odintsov, Phys. Rev. D **70**, 043539 (2004)
63. J.M. Cline, S. Jeon, G.D. Moore, Phys. Rev. D **70**, 043543 (2004)
64. A. Kamenshchik, U. Moschella, V. Pasquier, Phys. Lett. B **511**, 265 (2001)
65. M. Li, Phys. Lett. B **603**, 1 (2004)
66. M.C. Bento, O. Bertolami, A.A. Sen, Phys. Rev. D **70**, 083519 (2004)
67. M.C. Bento, O. Bertolami, A.A. Sen, Phys. Lett. B **575**, 172 (2003)
68. M. Makler, S. Quinet de Oliveira, I. Waga, Phys. Lett. B **555**, 1 (2003)
69. L. Amendola, F. Finelli, C. Burigana, D. Carturan, JCAP **0307**, 005 (2003)
70. H.B. Benaoum, arxiv:hep-th/0205140
71. J. Lu, L. Xu, J. Li, B. Chang, Y. Gui, H. Liu, Phys. Lett. B **662**, 87 (2008)
72. U. Debnath, A. Banerjee, S. Chakraborty, Class. Quant. Grav. **21**, 5609 (2004)
73. S. Silva e Costa, M. Ujevic, A. Ferreira dos Santos, Gen. Relativ. Grav.**40**, 1683 (2008)
74. L. Amendola, S. Tsujikawa, *Dark Energy: Theory and Observations* (Cambridge University Press, Cambridge, 2010), p. 172
75. S.D. Campo, R. Herrera, D. Pavon, J.R. Villanueva, JCAP **002**, 1008 (2010)
76. Y. Zhang, JCAP **023**, 0903 (2009)
77. A.R. Liddle, D.H. Lyth, Phys. Lett. B **291**, 391 (1992)
78. M. Czerny, T. Kobayashi, F. Takahashi, Phys. Lett. B **735**, 176 (2014)
79. E. Komatsu et al., Astrophys. J. Suppl. **192**, 18 (2011)
80. D. Larson et al., Astrophys. J. Suppl. **192**, 16 (2011)
81. G. Hinshaw et al., Astrophys. J. Suppl. **208**, 19 (2013)
82. P.A.R. Ade et al., arXiv:1502.01589